The microwave spectrum, structure, and large amplitude motions of the methylacetylene·SO_2 complex

Xue-Qing Tan, Li-Wei Xu, Michael J. Tubergen, and Robert L. Kuczkowski
Department of Chemistry, University of Michigan, Ann Arbor, Michigan 48109

(Received 6 June 1994; accepted 29 June 1994)

Rotational spectra of five isotopomers of the methylacetylene·SO_2 (MA·SO_2) van der Waals complex have been observed with a Fourier transform microwave spectrometer. Each species showed two sets of rotational transitions, one associated with the A ($m=0$) and the other with the E ($m=\pm 1$) methyl group internal rotation states. The rotational transitions of the isotopomers with S $^{16}O_2$ and the doubly substituted S $^{18}O_2$ also showed inversion splitting ranging from tens of kHz to a few MHz. This splitting was absent in the S ^{16}O ^{18}O isotopomers. The spectra of these species have been assigned and fit, yielding rotational constants, which allowed a complete determination of the structure of the complex. The SO_2 was found to sit above the carbon–carbon triple bond, with one of the S–O bonds roughly parallel to the symmetry axis of methylacetylene. The centers-of-mass distance between the two monomers was determined to be 3.382(10) Å. The center frequencies of the inversion doublets (or quartets) were used in a fit of both the A and the E transitions; the barrier hindering the internal rotation of the methyl group was determined to be 62.8(5) cm^{-1}. Based on the dependence of the inversion splitting on the transition dipole direction and isotopic substitution, the inversion motion was identified as an "in plane" wagging of the SO_2 relative to methylacetylene. A pure inversion splitting of 3.11 MHz (free from rotation) was extracted from the A-state spectrum of the normal species, from which an inversion barrier height of about 63 cm^{-1} was estimated.

I. INTRODUCTION

The fact that the sulfur atom in SO_2 has a relatively strong bonding interaction with the π system of small hydrocarbons is gradually being established through high resolution spectroscopy.[1–3] In ethylene·SO_2,[1] acetylene·SO_2,[2] and propene·SO_2,[3] the S atom was found to bind directly to the electron-rich double bond or triple bond of the hydrocarbons. The dimer configurations are all "stacked," with the plane of SO_2 and the small hydrocarbon close to parallel. SO_2 was also found to form relatively tight complexes with some aromatic systems such as benzene[4] and toluene.[5] In these complexes the interaction between the sulfur and the π electrons also seemed to be the dominate force that holds the monomers together. Besides the S-π electron interaction, a dipole–dipole interaction in some of these complexes has also been apparent. In propene·SO_2 (Ref. 3) and toluene·SO_2 (Ref. 5), the dipole moments of the two monomers in the complexes were observed to align more nearly antiparallel with each other. Also in these complexes, there are indications that one of the oxygen atoms in SO_2 is attracted to a methyl hydrogen. The relative importance of the latter two types of interactions in forming the complexes is of interest as an important aspect in the understanding of complex formation. These interactions can also influence the large amplitude internal motions in the complexes and, therefore, affect their dynamical behavior.

It is then a natural extension to the aforementioned studies of SO_2 and hydrocarbon dimer systems to investigate the rotational spectrum of the methylacetylene·SO_2 (MA·SO_2) complex. Methylacetylene has a significant dipole moment of 0.783 D, giving rise to a relatively strong dipole–dipole interaction when forming a complex with SO_2. In fact, there is even a possibility that the SO_2 will bond to the acetylenic hydrogen, forming a "linear" structure, as in SO_2·HF.[6] The methyl group in methylacetylene can also interact with an oxygen atom in SO_2, and remarkably, this interaction may manifest itself in the form of a potential barrier that hinders the internal rotation of the methyl group.

As will be seen later on, tunneling splitting caused by the SO_2 "in plane" rotation (or wagging) was also observed in the microwave spectrum of MA·SO_2. This kind of "inversion" splitting was not observed in acetylene·SO_2 (Ref. 2) and, therefore, is apparently influenced by the dipole–dipole interaction in MA·SO_2. The SO_2 inversion motion, the methyl group internal rotation, and the overall rotation of the complex generate a microwave spectrum with rich spectroscopic features. The large amplitude internal motions and the coupling between them are of considerable theoretical interest.

Complexes of methylacetylene with Ar, CO, and N_2 were recently studied by Blake *et al.*[7] and Lovas *et al.*[8] In these studies, the structures of the complexes were established. In the case of methylacetylene·Ar,[7] the barrier to internal rotation of the methyl group was also estimated to be about 11 cm^{-1}. Comparison of these results with the present study of MA·SO_2 could shed more light on the complexation properties of methylacetylene.

II. EXPERIMENT

The methylacetylene·SO_2 complex was generated in supersonic expansions, using a gas mixture of roughly 1% of methylacetylene, 1% of SO_2, and 98% of the "first run" Ne–He mixture (80% Ne and 20% He). The typical backing pressure is 1–2 atm. A Balle–Flygare type Fourier transform microwave spectrometer was used to observe the rotational transitions of MA·SO_2. The spectrometer operates between

 0021-9606/94/101(8)/6512/11/$6.00

7–18 GHz, with typical spectral linewidths ranging from about 30–50 kHz (Doppler limited). The digital frequency resolution of the spectrometer is 10 kHz, but usually the measured line positions are reproducible to within ±5 kHz.

The Stark effect was used to measure the dipole moments of the complex and to determine the J quantum numbers of unassigned rotational transitions. Stark effect measurements were also helpful in determining whether a particular rotational transition was associated with the A ($m=0$) or the E ($m=\pm 1$) torsional states. The spectrometer was equipped with two parallel steel mesh plates that were 30 cm apart and straddling the microwave cavity. dc voltages up to 9 kV were applied with opposite polarities to each plate. The electric field at each voltage was calibrated using the $J=1\leftarrow J=0$ transition of OCS (μ=0.715 196 D).[9]

S $^{18}O_2$ (99% ^{18}O) was purchased from Alfa. S $^{16}O^{18}O$ was prepared by mixing equal amount of S $^{18}O_2$ and S $^{16}O_2$. This mixture gives a ratio of 2:1:1 for $S^{16}O^{18}O$:$S^{18}O_2$:$S^{16}O_2$. CH_3CCD was prepared by mixing methylacetylene with D_2O in a 2 l glass bulb, placed in a heated oven (45 °C) for about six weeks.

III. RESULTS AND ANALYSIS

The frequency region of 8.4–9.5 GHz was scanned first in the initial search. Many transitions were observed. Most of these transitions were found to appear either as doublets, or as quartets. The splitting varies from less than a hundred kHz to a few MHz within a doublet or a quartet. Stark effect measurements were then conducted in order to determine the J quantum number of some of the transitions. It was then found that some of these transitions showed a second-order Stark effect, and others showed a first-order Stark effect. Since the transitions in each doublet or quartet have very similar Stark effects, the splitting is most likely caused by some kind of "inversion" motion. The transitions showing the second-order Stark effect were assumed to associate with the $m=0$ torsional state (the A lines) of MA·SO_2. These transitions are known[10] to show the usual asymmetric rotor behavior and therefore were assigned first. Initial fitting of these A-state transitions to the rigid rotor Hamiltonian yielded rotational constants for the complex. Predictions of A-state transitions in unsearched frequency regions were then made and subsequently confirmed. All of these transitions were found to be either a-type or c-type transitions. No b-type transitions were observed. Moreover, the inversion splitting of the a-type transitions was generally on the order of a few hundred kHz, while those of the c-type transitions was generally on the order of a few MHz. Altogether we found 35 A-line pairs (with $K_a\leqslant 2$) in the frequency region of 7.0–18.0 GHz; all of them appeared as doublets. The Watson A-reduction Hamiltonian[11] with quartic distortion terms was used to fit the center frequencies of these paired transitions. The standard deviation was 6 kHz, comparable to the experimental uncertainty of the measured line positions. The rotational constants obtained from such a fit, although contaminated by the methyl group internal rotation,[10] indicated that the two monomers in the complex are stacked on top of each other, and the C_2 axis of the SO_2 subunit points away from coplanar with the methylacetylene symmetry axis. The "linear" structure, with SO_2 bonded to the acetylenic hydrogen, was not observed, although its presence in the spectrum could not be rigorously excluded.

Next we measured the dipole moment of the complex, using the Stark effect. The splitting of five rotational transitions by the electric field were measured and used to calculate the dipole moment of MA·SO_2. The results were (in D), $\mu_a=0.921(1)$, $\mu_b=0.01(10)$, and $\mu_c=1.258(1)$. The b-dipole moment is indeed very small, which explains the absence of the b-type A-state transitions in the observed spectrum. The dipole moment information was then used to obtain an approximate structure of the complex. Here we assumed that the relative direction of the two monomer units was such that the calculated dipole moment components, obtained by summing the monomer dipole moment components, agree as closely as possible with the measured dipole moment components of the complex. The separation of the two subunits of the complex was then adjusted to match the fitted rotational constants. The resultant structure was subsequently used to predict the MA·S ^{16}O ^{18}O transitions. Many of the isotopomer lines were observed within ±25 MHz of the predicted frequencies, showing the usefulness of this crudely determined structure. Due to the nonequivalent positions of the two oxygen atoms in the complex, two sets of transitions, one for MA·S ^{16}O ^{18}O, the other for MA·S ^{18}O ^{16}O were observed.

Unlike the normal species, the rotational transitions of MA·S ^{16}O ^{18}O and MA·S ^{18}O ^{16}O did not show doublet or quartet structures, but rather appeared as singlet transitions. Thus the inversion splitting is "quenched" when one of the oxygen atoms in SO_2 is isotopically substituted. Again, we fit the A-state transitions of the isotopomers to the aforementioned Watson A-reduction Hamiltonian. The quality of the fits was excellent, with residual standard deviations less than 2 kHz for both isotopomers.

The structure of the complex could now be more accurately determined, since a total of nine rotational constants were known. If one assumes that the monomer structures do not change upon complexation, only five structural parameters are needed to specify the structure of the dimer (not counting the methyl group internal rotation angle, which cannot be determined). A structure fitting program, STRFTQ (Ref. 12), was used to fit the three sets of rotational constants. With all five parameters allowed to vary, a very decent fit, with standard deviation in the moment of inertia of about 0.05 amu Å^2, was obtained.

Due to the lightness of the methyl hydrogens, one can rotate the methylacetylene subunit by approximately 180° and get an equally good fit of the rotational constants. In the above procedure we used the dipole moment information to remove this ambiguity. Based on the known dipole moment directions of the two monomers, the methylacetylene was oriented in such a way that the two monomer dipole moments in the b-axis direction nearly cancel each other. Note, however, that the dipole moment direction in methylacetylene was determined in an indirect way.[13] Therefore, it is worthwhile to verify this result by deuterium substitution of the acetylenic hydrogen (*vide infra*).

The structure of the complex determined at this stage was also affected by the contamination of the rotational constants from the internal rotation of the methyl group, which could alter the A and B rotational constants by up to 15 MHz. Nevertheless, the fitted structure should still be a decent approximation of the real structure. We used this calculated structure to predict the A-state transitions of the MA·S $^{18}O_2$, and observed these transitions typically at frequencies within a few MHz of those predicted.

With this knowledge of the structure, the assignment of the E-state transitions was attempted. Here we used the complete torsion-rotation Hamiltonian, as described by Gordy and Cook,[10] and others,[5,7,14] to fit the A and E transitions simultaneously,

$$\mathscr{H}=AP_a^2+BP_b^2+CP_c^2+\mathscr{H}_d^{(1)}+\frac{1}{2}\sum_{i\neq j}^{a,b,c} D_{ij}(P_iP_j+P_jP_i)$$

$$-2\sum_{i}^{a,b,c} Q_iP_ip+Fp^2+V_3(1-\cos 3\alpha)/2+\mathscr{H}_d^{(2)}, \quad (1)$$

where

$$A=A_r+F\rho_a^2, \quad B=B_r+F\rho_b^2, \quad C=C_r+F\rho_c^2,$$

$$D_{ij}=F\rho_i\rho_j \quad (i,j=a,b,c,\ i\neq j),$$

$$Q_i=F\rho_i \quad (i=a,b,c),$$

$$F=F_0\left(1-\sum_{i}^{a,b,c}\rho_i\lambda_i\right)^{-1},$$

$$\rho_a=\frac{A_r}{F_0}\lambda_a, \quad \rho_b=\frac{B_r}{F_0}\lambda_b, \quad \rho_c=\frac{C_r}{F_0}\lambda_c.$$

A_r $(=\hbar^2/2I_a)$, B_r $(=\hbar^2/2I_b)$, and C_r $(=\hbar^2/2I_c)$ are rotational constants of the complex. $F_0=\hbar^2/2I_\alpha$, where I_α is the moment of inertia of the methyl group about its symmetry axis. λ_a, λ_b, and λ_c are direction cosines of the methyl group symmetry axis with respect to the principal axes of the complex. $\mathscr{H}_d^{(1)}$ contains the distortion terms in the usual Watson A-reduction Hamiltonian[11] (up to fourth order). $\mathscr{H}_d^{(2)}$ is the torsional state dependent distortion Hamiltonian,

$$\mathscr{H}_d^{(2)}=-D_{Jm}P^2p^2-D_{Km}P_a^2p^2-D_{K3m}P_a^3p$$
$$-d_{Km}[P_a(P_b^2-P_c^2)+(P_b^2-P_c^2)P_a]p$$
$$+d_mp^2(P_+^2+P_-^2)+2L_{Ja}P^2P_ap$$
$$+2L_{Jb}P^2P_bp+2L_{Jc}P^2P_cp. \quad (2)$$

A computer program was written to perform simulations and fitting for the aforementioned Hamiltonian. The combined basis functions $|JK\rangle\exp(im\alpha)$ were used to set up the Hamiltonian matrix. Here $|JK\rangle$ are the usual symmetric rotor basis functions; $\exp(im\alpha)$ are the torsional basis functions, with $m=3n+\sigma$, where $n=0, \pm1, \pm2,...$, $\sigma=0$ (for the A lines), and 1 (for the E lines). The complete Hamiltonian matrix was factored into two submatrices, one corresponds to $\sigma=0$, the other corresponds to $\sigma=1$. The torsional basis functions were truncated at $|n|\leq3$. It was tested that expanding the torsional basis functions to $|n|\leq4$ would not change the calculated torsion-rotation energies by more than 1 kHz (in this case). Rotational line strengths as well as the Boltzmann factor (for $T=1.5$ K) were calculated in the simulation program to predict the intensity of the experimental transitions. The terms involving D_{ij} were not included in the program since these terms generally have very little effect on the spectrum.

At the early stage of the analysis, the distortion terms in $\mathscr{H}_d^{(2)}$ were fixed at zero, and the values of the direction cosines were calculated from the determined structure. The threefold torsional barrier was then stepped at a 10 cm^{-1} interval. At each fixed V_3 value, the A-state transitions were fit first by varying the rotational constants and the distortion parameters in $\mathscr{H}_d^{(1)}$. The E-line frequencies were then predicted using the fitted parameters. It was hoped that an approximate match between the calculated and observed frequencies would occur at a certain value of V_3. However, no definitive match was found. Our next approach was to make assignments directly based on the Stark effect. Further searching had to be conducted in the frequency regions 11.0–11.5 GHz, and below 8.4 GHz since the number of existing transitions seemed to be insufficient to allow confident assignments. Additional strong E transitions were found, in particular the transitions near 8395 MHz (which showed the first order Stark effect of a $J=3\leftarrow J=2$ transition). With the added information, initial assignments were made for some E transitions. The frequencies of the assigned lines (about four or five of them at the beginning) were used in a fit to roughly determine V_3, which was found to be somewhere between 50–90 cm^{-1}. Large discrepancies between the calculated and the observed E-line frequencies still existed at this stage. We then allowed two of the direction cosines, namely λ_b and λ_c, to vary. This proved to be the crucial step since the standard deviation of the fit decreased dramatically, from tens of MHz to about 20 kHz.

The barrier from the fit was around 60 cm^{-1}, which can be considered as relatively low. It was then not surprising to see that the E-line spectrum was very sensitive to the direction cosines. The fitted direction cosines did not change too much from the values calculated from the structural determination, but the effect on the fit was significant. Once all the observed E lines were assigned and fit, new E-line positions in unsearched frequency regions were predicted. These new transitions were then measured, mostly within ±10 MHz of the predicted frequencies. The newly observed transitions were added to the assigned transitions and new fits were made to improve the Hamiltonian parameters. m dependent distortion terms were gradually added in to improve the fits. Altogether thirty-one E-state doublets or quartets were observed for the normal species.

Unlike the A lines, most E lines appear as quartets, due to the severe mixing of rotational basis functions of different symmetries (*vide infra*). In each quartet, the center of the middle two transitions coincide with the center of the outer two transitions. The center two transitions have roughly the same intensity, and the outer two transitions have roughly the same intensity. In principle, all the E lines should appear as

TABLE I. Observed microwave transitions (MHz) of methylacetylene·SO_2 (normal species, *A* lines).

J'	K_a'	K_c'	J''	K_a''	K_c''	ν_{obs}[a]	ν_{ave}[b]	Obs.-Cal.[c]
4	0	4	3	1	2	7255.719(+,−)	7257.060	−0.011
						7258.401(−,+)		
5	2	4	5	1	4	7393.911(−,+)	7395.227	−0.013
						7396.543(+,−)		
4	2	3	4	1	3	8149.199(−,+)	8150.556	0.002
						8151.912(+,−)		
3	1	3	2	1	2	8371.768(+,+)	8371.815	−0.005
						8371.862(−,−)		
3	2	2	3	1	2	8772.557(−,+)	8773.963	0.006
						8775.369(+,−)		
3	0	3	2	0	2	8781.098(−,−)	8781.281	−0.007
						8781.464(+,+)		
3	2	2	2	2	1	8879.692(+,+)	8879.853	0.001
						8880.015(−,−)		
3	2	1	2	2	0	8978.295(+,+)	8978.478	−0.027
						8978.662(−,−)		
5	0	5	4	1	3	9151.620(+,−)	9152.538	−0.004
						9153.456(−,+)		
2	2	1	2	1	1	9249.488(−,+)	9250.942	−0.008
						9252.396(+,−)		
3	1	2	2	1	1	9356.720(−,−)	9356.834	−0.011
						9356.947(+,+)		
2	1	1	1	0	1	9659.316(+,−)	9661.314	0.004
						9663.312(−,+)		
2	2	0	2	1	2	10 260.863(−,+)	10 262.140	0.026
						10 263.416(+,−)		
6	1	5	5	2	3	10 290.349(−,+)	10 291.767	0.019
						10 293.185(+,−)		
6	0	6	5	1	4	10 663.063(+,−)	10 663.527	−0.006
						10 663.991(−,+)		
3	2	1	3	1	3	10 867.756(−,+)	10 868.802	0.003
						10 869.848(+,−)		
4	1	4	3	1	3	11 135.639(+,+)	11 135.686	−0.006
						11 135.734(−,−)		
4	0	4	3	0	3	11 598.495(−,−)	11 598.734	−0.003
						11 598.972(+,+)		
4	2	2	4	1	4	11 793.165(−,+)	11 793.924	−0.002
						11 794.682(+,−)		
4	2	3	3	2	2	11 819.867(+,+)	11 820.068	−0.010
						11 820.269(−,−)		
4	2	2	3	2	1	12 060.568(+,+)	12 060.808	−0.010
						12 061.049(−,−)		
4	1	3	3	1	2	12 443.326(−,−)	12 443.477	−0.004
						12 443.628(+,+)		
5	2	3	5	1	5	13 116.517(−,+)	13 116.962	0.007
						13 117.408(+,−)		
3	1	2	2	0	2	13 121.190(+,−)	13 122.952	−0.001
						13 124.713(−,+)		
5	1	5	4	1	4	13 879.883(+,+)	13 879.922	−0.003
						13 879.962(−,−)		
5	0	5	4	0	4	14 338.682(−,−)	14 338.952	0.000
						14 339.223(+,+)		
5	2	4	4	2	3	14 743.277(+,+)	14 743.502	−0.006
						14 743.728(−,−)		
5	2	3	4	2	2	15 202.684(+,+)	15 202.958	0.004
						15 203.232(−,−)		
5	1	4	4	1	3	15 498.643(−,−)	15 498.829	0.008
						15 499.015(+,+)		
2	2	0	1	1	0	15 523.322(−,+)	15 524.696	0.009
						15 526.070(+,−)		
2	2	1	1	1	1	15 827.222(−,+)	15 828.542	−0.008
						15 829.862(+,−)		
6	1	6	5	1	5	16 603.220(−,−)	16 603.275	0.000
						16 603.330(+,+)		
4	1	3	3	0	3	16 783.715(+,−)	16 785.142	−0.004
						16 786.569(−,+)		
6	0	6	5	0	5	17 009.549(−,−)	17 009.816	0.004
						17 010.084(+,+)		
6	2	5	5	2	4	17 645.982(+,+)	17 646.214	−0.001
						17 646.447(−,−)		

[a]Observed transition frequencies. Also given (in parenthesis) are the inversion state assignments, (p',p''). When $p=$"+," the specified state is associated with the inversion state of positive parity (or symmetric species in group theoretical language). When $p=$"−," the specified state is associated with the inversion state of negative parity (or antisymmetric species).

[b]The average experimental frequencies of the inversion doublets.

[c]The differences between the averaged experimental frequencies (for the inversion doublets) and the corresponding calculated transition frequencies.

quartets. However, for some of them one of the two pairs have much smaller intensity and could not be observed, hence, these transitions appeared as doublets.

A total of seventy *A* lines (thirty-five averaged center positions) and one hundred and four *E* lines (thirty-one averaged center positions) were observed for the normal species. A fit of these sixty-six averaged center frequencies using Eq. (1) was conducted. The residual standard deviation was 14 kHz, quite acceptable considering the floppiness of the complex (the experimental uncertainty is about 5 kHz). The experimental transition frequencies of the normal species are reported in Tables I and II, along with the assignments and calculated frequencies. Note that the K_a and K_c quantum numbers assigned to the *E* lines were somewhat arbitrary due to the extensive mixing of the rotational basis functions with different K_a. The three direction cosines were found to strongly correlate with each other and could not be simultaneously fit. Therefore, λ_a was fixed in the fit but manually adjusted so that the sum of the squares of the three direction cosines was equal to 1 (within experimental error). The F_0 value was fixed at 5.308 352 cm^{-1}, which is the *A* rotational constant of methylacetylene determined by Graner *et al.*[15,16] The fitted molecular constants are reported in Table III.

With the information obtained from the normal species about the torsional motion, *E*-line searching became straightforward for the isotopically substituted species. We measured the *E*-state transitions for MA·$S^{16}O^{18}O$, MA·$S^{18}O^{16}O$, and MA·$S^{18}O_2$. The *A*- and *E*-state transitions of $CH_3CCD·SO_2$ (MA-d_1·SO_2) were also measured in order to determine experimentally the orientation of the methylacetylene subunit in the complex. Altogether, rotational transitions of five isotopomers (including the normal species) were measured and fit. The molecular constants of all these isotopomers are also reported in Table III. Experimental frequencies and the assignments of the four isotopically substituted species of MA·SO_2 can be found elsewhere.[17] In the case of $CH_3CCD·SO_2$, quadrupole splitting was only partially resolved for a few low *J* transitions. Therefore, we made no attempt to analyze the hyperfine structure of this species and used the average frequencies of the quadrupole components in the fit.

TABLE II. Observed microwave transitions (MHz) of methylacetylene·SO_2 (normal species, *E* lines).

J'	K_a'	K_c'	J''	K_a''	K_c''	ν_{obs}[a] (Inner pair)	ν_{obs}[b] (Outer pair)	ν_{ave}[c]	Obs.-Cal.[d]
3	1	3	2	1	2	8395.722	8394.881	8395.916	0.010
						8396.111	8396.949		
3	0	3	2	0	2	8418.530	8416.876	8418.546	0.024
						8418.564	8420.215		
2	1	2	1	0	1	8536.917	8535.691	8537.182	−0.001
						8537.447	8538.672		
3	2	1	2	2	0	8932.718		8932.860	0.015
						8933.001			
3	2	2	2	2	1	8960.964		8961.008	0.035
						8961.053			
2	2	1	2	1	2	9128.512	9127.286	9128.810	−0.015
						9129.107	9130.335		
3	1	2	2	1	1	9290.991	9290.566	9291.270	−0.006
						9291.549	9291.974		
4	2	2	4	1	3	9569.382	9569.104	9569.771	0.028
						9570.160	9570.437		
5	2	3	5	1	4	9583.402		9583.954	0.020
						9584.507			
3	2	2	3	1	3	9693.459	9692.621	9693.904	0.012
						9694.349	9695.186		
3	2	1	3	1	2	9827.416	9826.990	9827.916	0.004
						9828.416	9828.843		
2	2	0	2	1	1	10 185.962	10 184.979	10 186.326	−0.017
						10 186.689	10 187.672		
4	2	3	4	1	4	10 573.064	10 572.407	10 573.536	0.018
						10 574.010	10 574.665		
2	1	1	1	0	1	10 588.407	10 587.424	10 588.793	0.004
						10 589.179	10 590.161		
4	1	4	3	1	3	11 101.643	11 100.985	11 101.732	0.014
						11 101.822	11 102.480		
4	0	4	3	0	3	11 291.801	11 290.188	11 291.816	0.017
						11 291.831	11 293.446		
4	2	2	3	2	1	11 967.185		11 967.372	0.014
						11 967.559			
4	2	3	3	2	2	11 981.300		11 981.364	0.019
						11 981.428			
4	1	3	3	1	2	12 225.446	12 225.165	12 225.516	−0.011
						12 225.592	12 225.860		
3	2	1	3	1	3	12 774.587		12 774.882	−0.006
						12 775.176			
4	2	2	4	1	4	13 640.323		13 640.522	−0.006
						13 640.722			
5	1	5	4	1	4	13 854.440	13 853.871	13 854.486	0.009
						13 854.532	13 855.100		
5	0	5	4	0	4	14 102.613	14 101.077	14 102.647	0.002
						14 102.680	14 104.217		
3	1	2	2	0	2	14 343.098	14 342.671	14 343.731	−0.017
						14 344.365	14 344.788		
2	2	1	1	1	1	14 873.227	14 871.529	14 873.287	−0.009
						14 873.347	14 875.044		
5	2	4	4	2	3	14 957.994		14 958.073	−0.027
						14 958.152			
5	1	4	4	1	3	15 060.106	15 059.828	15 060.192	0.011
						15 060.279	15 060.557		
5	2	3	4	2	2	15 074.078		15 074.328	−0.043
						15 074.578			
2	2	0	1	1	0	16 380.257	16 378.642	16 380.304	−0.017
						16 380.349	16 381.967		
6	1	6	5	1	5	16 632.862		16 632.898	−0.025
						16 632.935			
6	0	6	5	0	5	16 818.372	16 816.981	16 818.444	−0.009
						16 818.515	16 819.907		

[a]Observed transition frequencies of the inner pair of the quartets.
[b]Observed transition frequencies of the outer pair of the quartets.
[c]The average experimental frequencies of the inversion quartets or doublets.
[d]The differences between the averaged experimental frequencies (for the quartets or doublets) and the corresponding calculated transition frequencies.

IV. DISCUSSION

A. Structure and dipole moment

As expected, MA·SO_2 was observed to have a "stacked" structure. In this configuration, the relative positions of the two subunits in the complex can be specified by one distance and five angles. These are the distance between the centers of mass (COM) of the two monomers, the methyl group internal rotation angle, the angle between the symmetry axis of methylacetylene, and the line joining the COM ($\angle C_3X_1X_2$, cf. Fig. 1), the SO_2 tilt angle ($\angle SX_2X_1$), the dihedral angle that specifies the "in plane" rotation of the SO_2 subunit relative to methylacetylene ($\angle SX_2X_1C_3$), and the dihedral angle that specifies rotation of the SO_2 with respect to its own C_2 axis ($\angle O_ASX_2X_1$). Among the five angles, the equilibrium methyl group internal rotation angle could not be determined experimentally since the moments of inertia are insensitive to changes in this angle. The other structural parameters were determined by a fit to the rotational constants of the five isotopomers of the complex. Again Schwendeman's computer program[12] STRFTQ was used to do the fitting and we assumed that the monomer structures were unchanged in the complex. The literature values of the monomer geometries were used.[18] All fifteen rotational constants listed in Table III were included. A rather satisfactory fit was obtained, with a standard deviation in the moment of inertia of 0.074 amu Å^2. Schematic diagrams of the determined structure viewed from the side and the top are shown in Figs. 1(a) and 1(b), respectively. The aforementioned structural parameters and the Cartesian coordinates of the atom positions in the principal axis system are reported in Tables IV and V. As can be seen in Fig. 1, the S atom in SO_2 is situated above the carbon–carbon triple bond. One S–O bond points in the direction of the methyl group and is nearly parallel to the methylacetylene symmetry axis. The other S–O bond stems out of the plane established by the S atom and the methylacetylene symmetry axis. The COM distance between SO_2 and methylacetylene was determined to be 3.3816(2) Å.

In the reported COM distance and other parameters in Table IV, the uncertainty was quoted from the output of the fitting program. It is not clear how meaningful this estimate of error is, since the monomer structures have uncertainties which propagate. Perhaps more importantly, the floppy nature of a weakly bound complex makes it difficult to estimate how the observed vibrationally averaged moments of inertiae are related to an equilibrium geometry. Based on these considerations, it is perhaps more realistic to use 0.01–0.02 Å as the uncertainty of the COM distance of MA·SO_2, with similar scaling in the other parameters when trying to relate them to the equilibrium structure.

The separation between the two monomers in MA·SO_2 seems to be closely related to the van der Waals radii of relevant atoms. In the experimental structure, the distance between the sulfur atom and the closest carbon atom (C2 in Fig. 1) is 3.34 Å, very close to the sum of the van der Waals radii of sulfur and carbon, which is 3.5 Å from Bondi's tabulation.[19] The closest distance between an oxygen and a methyl hydrogen is about 2.5 Å. This distance also compares

TABLE III. Molecular constants of methylacetylene·SO_2 (MA·SO_2) and its isotopomers. The numbers in parenthesis are 1 standard deviation. For the meaning of the parameters, see Eqs. (1) and (2). F_0 was fixed in the fits at 5.308 352 cm^{-1}. The number of digits retained in this table typically will not allow an accurate reproduction of the calculated frequencies listed in Tables I and II. For a listing of these parameters with more digits, see Ref. 17.

	MA·SO_2	MA·$S^{18}O^{16}O$[a]	MA·$S^{16}O^{18}O$[b]	MA·$S^{18}O_2$	MA-d_1·SO_2
A_r (MHz)	4716.223 (8)	4623.836 (9)	4562.975 (9)	4470.573 (9)	4455.027 (10)
B_r (MHz)	1638.948 (10)	1601.167 (16)	1631.086 (13).	1594.763 (13)	1629.130 (13)
C_r (MHz)	1317.143 (12)	1291.746 (18)	1300.360 (15)	1275.658 (15)	1290.224 (15)
Δ_J (kHz)	3.54 (3)	3.42 (4)	3.37 (3)	3.34 (3)	3.25 (5)
Δ_{JK} (kHz)	3.1 (1)	2.3 (2)	3.8 (2)	2.8 (2)	5.4 (4)
Δ_K (kHz)	13.2 (14)	18.1 (16)	12.5 (16)	15.2 (16)	9.4 (20)
δ_J (kHz)	0.41 (1)	0.33 (2)	0.41 (2)	0.37 (2)	0.43 (2)
δ_K (kHz)	12.9 (6)	10.2 (13)	9.6 (10)	10.3 (10)	7.1 (15)
V_3 (cm^{-1})	62.8 (5)	62.9 (6)	63.4 (6)	63.2 (6)	63.0 (7)
λ_a[c]	0.295	0.306	0.286	0.296	0.279
λ_b	0.939 (2)	0.931 (2)	0.948 (2)	0.934 (2)	0.942 (2)
λ_c	0.204 (4)	0.219 (5)	0.208 (4)	0.222 (3)	0.190 (3)
D_{Jm} (MHz)	1.589 (1)	1.568 (1)	1.511 (1)	1.541 (1)	1.457 (1)
D_{km} (MHz)	−6.056 (2)	−6.037 (2)	−5.615 (2)	−5.576 (2)	−5.502 (3)
D_{K3m} (MHz)	−0.223 (11)	−0.211 (14)	−0.216 (14)	−0.206 (13)	−0.226 (15)
d_m (MHz)	−0.099 (4)	−0.086 (6)	−0.070 (5)	−0.094 (5)	−0.118 (5)
d_{Km} (MHz)	0.68 (8)	0.82 (12)	0.67 (10)	0.65 (10)	0.64 (11)
L_{Ja} (MHz)	−0.064 (4)	−0.051 (5)	−0.060 (5)	−0.053 (5)	−0.064 (5)
L_{Jb} (MHz)	0.039 (2)	0.038 (2)	0.039 (1)	0.037 (1)	0.037 (1)
L_{Jc} (MHz)	0.009 (1)	0.010 (1)	0.010 (1)	0.010 (1)	0.009 (1)
n[d]	66	56	58	59	47
$\Delta\nu_{rms}$[e] (kHz)	14	9	10	9	12

[a] O_B (see Fig. 1) is substituted by an ^{18}O in this isotopomer.
[b] O_A (see Fig. 1) is substituted by an ^{18}O in this isotopomer.
[c] λ_a was manually adjusted in the fits so that $\lambda_a^2+\lambda_b^2+\lambda_c^2\approx 1$ (within experimental error).
[d] Number of observed transitions, or averaged center frequencies included in the fit.
[e] $\Delta\nu=\nu_{obs}-\nu_{cal}$.

well with the sum of the van der Waals radii of oxygen and hydrogen (2.7 Å).[19] These observations suggest that MA·SO_2 is a fairly tight complex and that a significant attractive force exists between the two monomers of the complex.

Compared to the observed structure of acetylene·SO_2,[2] in which the C_2 axis of the SO_2 was found to be perpendicular to acetylene, the SO_2 subunit in MA·SO_2 is rotated by about 30° from that in acetylene·SO_2. This rotation is consistent with a dipole–dipole interaction in MA·SO_2, which tends to align the dipole moments of SO_2 and methylacetylene antiparallel. There also may be an attractive interaction between the oxygen atom near the methyl group and the methyl hydrogens, since one S–O bond is directed toward the methyl group. This latter interaction may also prevent the SO_2 subunit from further rotating to align the two dipole moments even closer antiparallel. The COM distance between acetylene and SO_2 in acetylene·SO_2 was determined to be 3.430(1) Å, only slightly larger than the 3.382 Å COM distance between methylacetylene and SO_2. So despite the added dipole–dipole and O···H interactions in MA·SO_2, the two complexes probably have similar stabilities.

Many other related dimer species were observed to have structures similar to MA·SO_2. Methylacetylene·CO and methylacetylene·N_2 were both found[8] to have "stacked," or

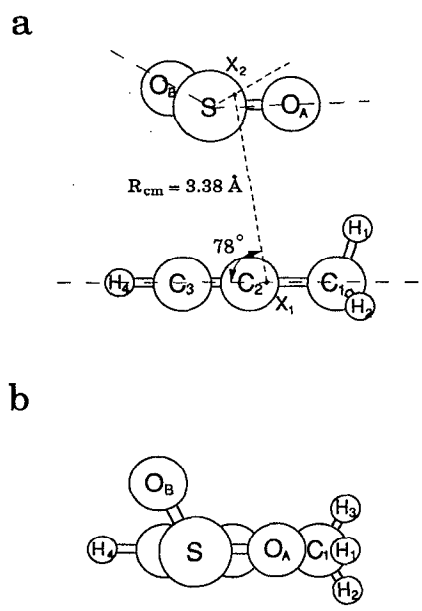

FIG. 1. Schematic diagram of the structure of the methylacetylene·SO_2 complex. (a) Viewed from the "side." X_1 and X_2 are the center of masses of the methylacetylene and SO_2 monomers, respectively. (b) Viewed from the "top."

TABLE IV. Structural parameters of methylacetylene·SO_2. For the definition of the structural parameters, see text and Fig. 1. The distance is in angstroms, the angles are in degrees. The numbers in parenthesis are one standard deviation (from the output of STRFTQ). The sign of the two dihedral angles is consistent with the definition in Ref. 30.

$d(X_1-X_2)$	$\angle C_3X_1X_2$	$\angle SX_2X_1$	$\angle SX_2X_1C_3$	$\angle O_ASX_2X_1$
3.3816 (2)	77.81 (27)	86.48 (99)	58.36 (43)	73.53 (25)

the so-called "slipped parallel" structure, with the diatomic approximately over the triple bond. In methylacetylene·CO, the dipole moments of the two monomers were also found to align roughly antiparallel with each other. In both complexes, the COM distances between the two subunits are larger than 3.7 Å, indicating that they are both less strongly bound than MA·SO_2. Ethylene·SO_2 and propene·SO_2 were also observed[1,3] to be "stacked." Ethylene·SO_2 seems to be less strongly bound than MA·SO_2, since the COM distance between ethylene and SO_2 increases[1] to 3.504 Å. However, the COM distance between propene and SO_2 in propene·SO_2 is 3.26 Å,[3] indicating that propene is perhaps more strongly bound to SO_2 than methylacetylene.

Based on the determined structure of MA·SO_2 and the dipole moments of the two monomers, the dipole moment components of the complex can be estimated (neglecting the induction effects). Here, the projections of the two monomer dipole moments on each complex principal axis were summed, giving (in D) $\mu_a=0.299$, $\mu_b=0.166$, and $\mu_c=1.374$. Compared to the dipole moments measured using the Stark effect, $\mu_a=0.921(1)$, $\mu_b=0.01(10)$, and $\mu_c=1.258(1)$, only μ_a shows a substantial difference between the calculated and the measured values. This is not surprising since strong mutual polarization in the direction that joins the two monomers is often observed in complex formation. This polarization effect in MA·SO_2 is similar to that in toluene·SO_2, where the increase in μ_a is 0.61 D, but is greater than that in acetylene·SO_2, where $\Delta\mu_a=+0.33$ D. Since the calculated μ_b is close to that observed in the experiment, the present study also verified the direction of the dipole moment in methylacetylene (the methyl group is at the positive end), experimentally determined by Muenter and Laurie[13] indirectly using vibrational effects on the dipole moment upon deuteration.

TABLE V. The Cartesian coordinates of the atom positions in the principal axis system of methylacetylene·SO_2 (Å).

Atom[a]	X_a	X_b	X_c
C1	2.483	−0.956	0.284
C2	2.014	0.393	−0.014
C3	1.627	1.508	−0.261
H1	1.624	−1.643	0.399
H2	3.126	−1.327	−0.535
H3	3.067	−0.959	1.222
H4	1.288	2.484	−0.477
S	−1.282	−0.031	−0.351
O_A	−0.818	−1.353	−0.048
O_B	−1.788	0.797	0.705

[a]The labeling of the atoms is illustrated in Fig. 1.

B. Inversion motion

The inversion splitting is one of the interesting observations made in the present study. The magnitude of the inversion splitting was found to depend on the dipole selection rule, isotopic substitution, and the torsion-rotation state. Based on the structure of the complex, three possible internal motions may be proposed to account for the inversion splitting. First the off-plane oxygen (O_B in Fig. 1) can "flip over" from one side of methylacetylene to the other [from pointing into the paper to out of the paper, as in Fig. 1(a)]; second, the SO_2 subunit can rotate around its local C_2 axis by 180°; third, a relative rotation (or wagging motion) between the two monomers roughly about the line that joins the COM moving SO_2 to the equivalent position on the other side of methylacetylene. The isotopic dependence, i.e., a "quenching" of the inversion splitting when one of the oxygen atoms in SO_2 is isotopically substituted, indicates that an exchange of the two oxygen atoms in SO_2 is involved in the "inversion" motion. Therefore, the first type of internal motion can be eliminated. The second type of internal motion is not likely to happen from chemical intuition, but a more conclusive argument can be made using the transition dipole selection rule. As will be shown later, the *c*-dipole transitions connect inversion levels with different parity (or symmetry), so the inversion motion reverses the direction of the *c*-dipole moment of the complex. Since a rotation of the SO_2 around its C_2 axis does not reverse the direction of the *c*-dipole moment, it is therefore not responsible for the inversion splitting. Thus the "inversion" motion can be identified as a relative rotation between the two monomers along the vertical direction [Fig. 1(a)]. This kind of internal motion has also been observed in some other SO_2 containing complexes, such as ethylene·SO_2 (Ref. 1) and toluene·SO_2 (Ref. 5), although in the latter case, the "flip over" motion could not be excluded. It is interesting that the "inversion" splitting was not observed in acetylene·SO_2.[2] It may be that this is related to the absence of a favorable dipole–dipole interaction like that in MA·SO_2, which could reduce the inversion barrier height.

In assigning the inversion transitions it is necessary to first make assumptions about the dipole selection rules. Based on the observation that the inversion splitting was generally small for the *a*-type rotational transitions, it is reasonable to assume that the inversion levels connected by the *a*-dipole have the same parity, as is shown in Fig. 2(a). We also assume that the inversion levels connected by the *c* dipole have opposite parity, as is shown in Fig. 2(b). Having different selection rules for the *a* and the *c* dipoles allows one to explain the quartet structure observed for the *E*-state rotational transitions. The quartet structure resulted from all four transitions between the two upper state inversion levels and the two lower state inversion levels being allowed, as is shown in Fig. 2(c). Rotational transitions between two *E*-state levels can be connected by both the *a* and the *c* dipoles due to the extensive torsion-rotation coupling.

Based on these selection rules, the *A*-state rotation-inversion transitions of the normal species were tentatively assigned. In this process, the "combination sum" check was used to help the assignment. The procedure is illustrated in

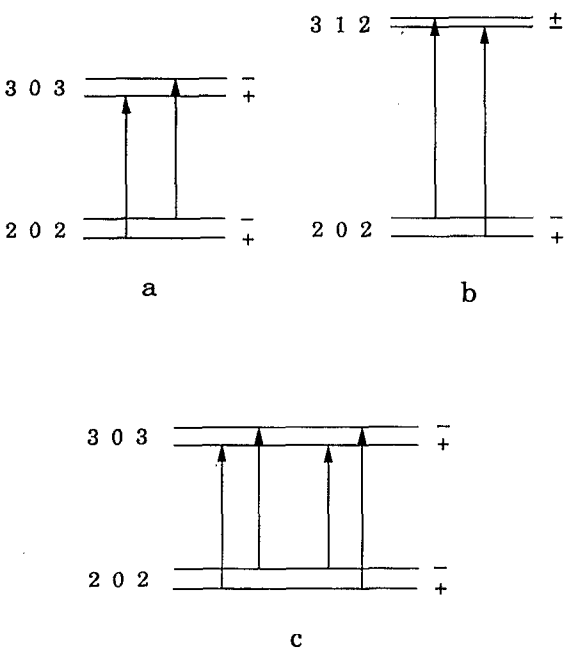

FIG. 2. Schematic diagram of rotational transitions of MA·SO_2, showing the inversion levels connected by the *a*- and the *c*-dipole moments. (a) *a*-type, *A*-state transitions. The inversion levels connected by the *a*-dipole moment have the same parity. (b) *c*-type, *A*-state transitions. The inversion levels connected by the *c*-dipole moment have different parities. (c) *E*-state transitions. Each rotational transition is connected by both the *a* and the *c* dipoles.

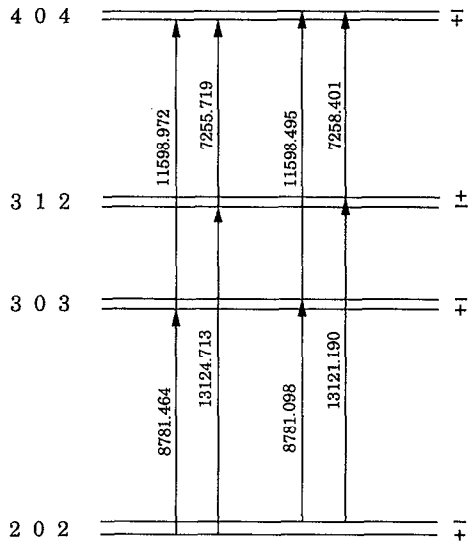

FIG. 3. Schematic diagram showing the "combination sums." The frequency sums, 8781.464+11 598.972=20 380.436 and 13 124.713 +7255.719=20 380.432 agree with each other within experimental error. Hence the transitions 8781.464 and 13 124.713 should originate from the same inversion level (the "+" level). The transitions 11 598.972 and 7255.719 should end on the same inversion level (also the "+" level). Following similar arguments, the transitions 8781.098 and 13 121.190 should originate from the same inversion level (the "−" level), and the transitions 11 598.495 and 7258.401 should end on the same inversion level (the "−" level).

Fig. 3. Assuming that the two inversion states have independent rotational and distortion constants, the *A*-state rotation-inversion transitions of the normal species can be satisfactorily fit to the Watson *A*-reduction Hamiltonian. The standard deviation of the fit was 12 kHz. The successful fit indicates that the assumed dipole selection rules for the inversion transitions are correct. A pure inversion splitting of 3.11(1) MHz (at zero rotational energy) was also obtained in the fit. This is the splitting that is caused by the tunneling through the inversion barrier. The inversion assignments of the *A*-state transitions of the normal species are given in Table I. Similar fits of the *A*-state rotation-inversion transitions were also obtained for MA·$S^{18}O_2$ and MA-d_1·SO_2. The pure inversion splitting for the two isotopomers was determined to be 1.94(1) and 2.14(1) MHz, respectively. We used the same procedure to try to assign and fit the *E*-state rotation-inversion transitions to the Hamiltonian described in Eq. (1) but were not very successful. The standard deviation of the best trial fit was larger than 100 kHz. This is not surprising since a significant coupling between the inversion motion and the methyl group internal rotation can be expected. It is perhaps possible to fit the *E*-state rotation-inversion transitions to roughly the experimental accuracy using a more sophisticated approach.[20] Such a possibility will be explored in the future.

A crude estimate of the inversion barrier height can be made by solving the following one-dimensional-rotor Hamiltonian

$$H_{\text{inv}} = -F\frac{\partial^2}{\partial\phi^2} + V_{\text{inv}}(\phi),$$

where $F=0.5792$ cm^{-1} (for the normal species) is the sum of the *C* rotational constant of SO_2 and the *B* rotational constant of methylacetylene; $V_{\text{inv}}(\phi)$ is the inversion potential and can be approximated by the first two terms of a Fourier expansion

$$V_{\text{inv}}(\phi) = V_1(1-\cos\phi)/2 - V_2(1-\cos 2\phi)/2$$

ϕ is the "in-plane" rotation angle, $\phi=0°$ corresponds to SO_2 symmetrically straddling the symmetry axis of methylacetylene and the oxygen atoms pointing toward the methyl group. Assuming that the minima of $V_{\text{inv}}(\phi)$ are at $\phi=\pm 60°$, which are approximately the two equivalent equilibrium positions of the SO_2 in the experimental structure, it can be easily shown that $V_1=2V_2$. V_1 can then be obtained by matching the calculated inversion splitting with that observed in the experiment. Setting up the Hamiltonian matrix with the free rotor basis functions $\exp(im\phi)$, we found that when $V_1=2V_2=503$ cm^{-1}, the calculated inversion splitting is equal to 3.12 MHz, similar to that obtained from the experiment (3.11 MHz). The inversion barrier height is then about 63 cm^{-1}. Using the same inversion potential, we also calculated the inversion splitting of MA·$S^{18}O_2$ and MA-d_1·SO_2, for which *F* is equal to 0.5482 and 0.5533 cm^{-1}, respectively. The results are, 2.07 MHz for MA·$S^{18}O_2$ and 2.22 MHz for MA-d_1·SO_2, both compare favorably with the corresponding experimental values of 1.94 and 2.14 MHz.

TABLE VI. Comparison of the direction cosines of the methyl group in MA·SO_2 determined from the spectral fit and from the structure (normal species).

	λ_a	λ_b	λ_c
From the fit	0.295	0.939	0.204
From the structure	0.321	0.925	0.204

C. Internal rotation of the methyl group

Internal rotation motions in molecular complexes have generated perhaps some of the most complicated rotational spectra.[4,21,22] In the case of MA·SO_2, all the ingredients exist for a microwave spectrum that is extremely difficult to analyze. Fortunately, accurate structural information, as well as the knowledge of certain rotational quantum numbers from the Stark effect, allowed an assignment of this spectrum. The torsional barrier determined for the ground electronic state of this complex is 62.8(5) cm^{-1}, somewhere between the low barrier limit and the intermediate barrier limit. The quality of the simultaneous fit of both the *A* lines and the *E* lines is quite decent, as the residual standard deviation is on the same order of magnitude as the experimental uncertainty. In addition, the internal rotation dependent distortion constants for various isotopomers of MA·SO_2 are all quite consistent with each other, indicating the suitability of the distortion Hamiltonian used in the current analyses.

As can be seen in Table VI, the direction cosines obtained from the fit, with the constraint that the sum of their squares equals 1, are not very different from the ones calculated from the determined structure of the complex. The deviations correspond to differences in angles of about 2°. Considering the floppiness of the complex, one can easily attribute the differences to the uncertainty in the structure. There is, however, another possible cause for the apparent disagreement of the direction cosines. Due to the weakness of the bonding between the two monomers in the complex, the methyl group may very well execute a wobbling type of motion.[23] Therefore, the fitted direction cosines may be different from the ones calculated from the structure (even though the structure is accurate). If this is indeed the case, the uncertainty of the torsional barrier height may be much larger (± 5 cm^{-1}, for example) than that indicated in Table III.

Comparisons of the current torsional analysis with those for related systems can be made. In methylacetylene·Ar, the torsional barrier was estimated[7] to be about 11 cm^{-1}, significantly smaller than that in MA·SO_2. The magnitudes of the internal rotation dependent distortion constants, however, are quite comparable. This may be the result of the similar structures for the two complexes. Preliminary results also showed that methylacetylene·N_2 and methylacetylene·CO have torsional barriers of $\leqslant 10$ and ~ 30 cm^{-1}, respectively.[24] In the case of toluene·SO_2, the barrier to internal rotation of the methyl group was determined[5] to be 83 cm^{-1}, i.e., 20 cm^{-1} larger than that in MA·SO_2. Since the SO_2 is further away from the methyl group in toluene·SO_2, this increased torsional barrier is most likely caused in large part by the perturbation of the ring electron distribution by the SO_2. Such a perturbation may create an imbalance on the two sides of the ring adjacent to the methyl group, and induce a large torsional barrier. The internal rotation related distortion constants for toluene·SO_2 are generally much smaller than the corresponding ones in MA·SO_2, suggesting that toluene·SO_2 is a more tightly bound complex.

The origin of the torsional barrier in MA·SO_2 is also of considerable interest. As previously discussed, one S–O bond is oriented toward the methyl group. This suggests that there might be a bondinglike interaction between the oxygen and a methyl hydrogen. This interaction can certainly contribute to the torsional barrier. Steric hindrance is another possible contributor to the torsional barrier in MA·SO_2. Since the steric effect is often repulsive in nature, it could partially cancel the torsional barrier generated by the O···H attractive interaction. One can get some idea of the likely magnitude of the steric hindrance from the torsional barrier measured in methylacetylene·Ar,[7] where $V_3 \sim 11$ cm^{-1}. Moreover, the steric effect was believed to be responsible for torsional barrier heights of about 40 cm^{-1} in 2-naphthol·NH_3.[21] On the other hand, a bonding interaction between an oxygen atom and a methyl hydrogen potentially may have a much larger effect on the torsional barrier height. In the case of 2-pyridone·NH_3, the barrier to internal rotation of ammonia was found[25] to be 424 cm^{-1}. This unusually high torsional barrier is caused by a hydrogen bond between an ammonia hydrogen and the carbonyl oxygen of the 2-pyridone. In light of these observations, we believe that the torsional barrier in MA·SO_2 is probably generated mostly by the O···H attraction. Steric effect may slightly reduce this barrier, resulting in a net torsional barrier of 63 cm^{-1}. Incidentally, the estimated inversion barrier height is almost the same as this torsional barrier height, so it is quite possible that the O···H interaction is also an important factor in determining the inversion barrier.

D. Electrostatic modeling

Electrostatic modeling has been found to successfully rationalize the qualitative structures of many van der Waals complexes.[26] The structures of many small hydrocarbon complexes [including methylacetylene·N_2, (Ref. 8), methylacetylene·CO (Ref. 8), acetylene·SO_2 (Ref. 2), propene·SO_2 (Ref. 3), and butadiene·SO_2 (Ref. 27)] have been modeled using this approach. The procedure involves representing the electric field of the constituent monomers by a series of multipole moments. Polarization terms are neglected in this calculation, so the induced dipole contributions to the energy are not included. Moreover, the quality of the calculation depends on the *ab initio* basis set and computational level used to calculate the molecular electric field. For complexes where the electrostatic terms dominate the polarization terms (such as those formed by hydrogen bonding or dipole–dipole interactions), this model seems to be rather useful in predicting the structures.

The method of Buckingham and Fowler[26] was used to estimate the electrostatic interaction between the monomers as a function of their relative orientation. Distributed multipoles (up to the quadrupole moments; available as supplementary material[17]) for methylacetylene were calculated

from the 6-31G** basis set using the Cambridge analytic derivatives package;[28] the multipoles for SO_2 were taken from the literature.[26] Two structures were initially considered: the experimentally determined structure and a "*cis* hydrogen-bonded" form, which is a likely structure if the acetylenic hydrogen forms a hydrogen bond to the SO_2. The electrostatic calculations found that the experimental structure is more stable than the hydrogen-bonded form—with the binding energies estimated to be 1380 and 940 cm^{-1}, respectively. Similar results were obtained using previously published multipole moments for methylacetylene.[8]

Similar calculations were performed to model the electrostatic potential along two internal motion pathways. For internal rotation of the methyl group a barrier of 160 cm^{-1} was found. The minimum energy configuration has one methyl hydrogen directed toward the nearest SO_2 oxygen. This result is consistent with an attractive interaction between the methyl hydrogens and the nearby SO_2 oxygen. The second internal motion is the tunneling motion of SO_2, which we approximated as an in-plane wagging motion exchanging the SO_2 oxygen atoms. A dihedral angle of ~80° between the symmetry axes of the SO_2 and methylacetylene was found for the minimum energy structure along this path (the experimental value is ~60°, such that an S–O bond is nearly parallel to the methylacetylene axis). Thus the electrostatic calculations do not exactly reproduce the experimental structure. A barrier to wagging of 120 cm^{-1} occurs when both oxygen atoms are oriented towards the methyl groups and the two monomer symmetry axes are parallel. Not surprisingly, the maximum barrier occurs when the two monomer dipoles are parallel (oxygen atoms directed away from the methyl group).

As was found for many other hydrocarbon·SO_2 complexes, the electrostatic calculations qualitatively reproduce the experimental observations for methylacetylene·SO_2. Perhaps the most striking feature of these calculations is that they favor the "stacked" structure over the hydrogen bonded structure. Electrostatic modeling of the acetylene·SO_2 and HCN·SO_2 complexes[2,26] favored hydrogen bonded structures, but rotational spectra were found only for a stacked acetylene·SO_2 complex[2] and an "anti-hydrogen-bonded" HCN·SO_2 complex.[29] The observation that the experimental structure of methylacetylene·SO_2 is modeled reasonably well by the electrostatic calculations suggests that the dipole–dipole interaction (and other electrostatic interactions) is significant in determining the structure of the complex.

V. CONCLUSION

In conclusion, the microwave spectra of methylacetylene·SO_2 and four of its isotopomers were observed. Rotational analysis yielded rotational constants of these species, which led to the determination of the structure of the complex. MA·SO_2 was found to have a stacked structure, with a centers-of-mass distance of 3.382(10) Å between the two monomers. The observed structure of MA·SO_2 is consistent with the postulate that there is a significant bondinglike interaction between the sulfur and the π system of some hydrocarbons. The dipole moment of MA·SO_2 was measured using the Stark effect. A fairly large *a*-dipole moment was observed, implying a significant induced dipole moment between the two monomers. The *b*-dipole moment was found to be almost equal to zero, so the dipole moments of the two monomers are aligned closer to antiparallel with each other. Electrostatic calculations based on the distributed multipole method can qualitatively reproduce the experimental geometry of the complex, so the dipole–dipole, and other multipole interactions appear to be important in determining the relative orientation of the two monomers in the complex. Spectral splittings associated with both the internal rotation of the methyl group and the inversion motion of the SO_2 were observed. Analysis of the internal rotation of the methyl group was conducted. The torsional barrier was determined to be 62.8(5) cm^{-1}. This barrier is believed to be caused mostly by an attractive interaction between an oxygen in SO_2 and a methyl hydrogen. The inversion pathway was identified as an "in-plane" rotation (or wagging) of the SO_2 subunit relative to methylacetylene. A pure inversion splitting of 3.11(1) MHz (for the normal species) could be extracted from a fit to the *A*-state rotation-inversion transitions using simple theoretical models. From this value an estimated inversion barrier of 63 cm^{-1} was obtained. The present work extended our knowledge about the structure, bonding, and the dynamics of the SO_2 containing weakly bound complexes, especially regarding the dipole–dipole interaction and the large amplitude internal motions. The results obtained in the present work should be valuable for theoretical modeling and calculations.

ACKNOWLEDGMENTS

This work was supported by the National Science Foundation, Washington, D.C. The authors are grateful to the donors of the Petroleum Research Fund, administered by the American Chemical Society, for the support of this work. We are grateful for an allotment of computing time at the San Diego Supercomputing Center. We thank Professor D. F. Eggers for information on the barriers in methylacetylene·N_2 and methylacetylene·CO prior to publication.

[1] A. M. Andrews, A. Taleb-Bendiab, M. S. LaBarge, K. W. Hillig II, and R. L. Kuczkowski, J. Chem. Phys. **93**, 7030 (1990).
[2] A. M. Andrews, K. W. Hillig II, R. L. Kuczkowski, A. C. Legon, and N. W. Howard, J. Chem. Phys. **94**, 6947 (1991).
[3] L.-W. Xu and R. L. Kuczkowski, J. Chem. Phys. **100**, 15 (1994).
[4] A. Taleb-Bendiab, K. W. Hillig II, and R. L. Kuczkowski, J. Chem. Phys. **97**, 2996 (1992).
[5] A. Taleb-Bendiab, K. W. Hillig II, and R. L. Kuczkowski, J. Chem. Phys. **98**, 3627 (1993).
[6] A. J. Fillery-Travis and A. C. Legon, J. Chem. Phys. **85**, 3180 (1986).
[7] T. A. Blake, D. F. Eggers, S.-H. Tseng, M. Lewerenz, R. P. Swift, R. D. Beck, R. O. Watts, and F. Lovas, J. Chem. Phys. **98**, 6031 (1993).
[8] F. J. Lovas, P. W. Fowler, Z. Kisiel, S.-H. Tseng, R. D. Beck, D. F. Eggers, T. A. Blake, and R. O. Watts, J. Chem. Phys. **100**, 3415 (1994).
[9] K. Tanaka, H. Ito, K. Harada, and T. Tanaka, J. Chem. Phys. **80**, 5893 (1984).
[10] W. Gordy and R. L. Cook, *Microwave Molecular Spectra*, 3rd. Ed. (Wiley-Interscience, New York, 1984).
[11] J. K. G. Watson, in *Vibrational Spectra and Structure*, edited by J. Durig (Elsevier, Amsterdam, 1977), Vol. 6.
[12] R. H. Schwendeman, in *Critical Evaluation of Chemical and Physical Structural Information*, edited by D. R. Lide and M. A. Paul (National Academy of Sciences, Washington, D.C., 1974), pp. 94–115.

[13] J. S. Muenter, V. W. Laurie, J. Chem. Phys. **45**, 855 (1966).
[14] F. Rohart, J. Mol. Spectros. **57**, 301 (1975).
[15] G. Graner, J. Demaison, G. Wlodarczak, R. Anttila, J. J. Hillman, and D. E. Jennings, Mol. Phys. **64**, 921 (1988).
[16] A. McIllroy and D. J. Nesbitt, J. Chem. Phys. **91**, 104 (1989).
[17] See AIP document No. PAPS JCPSA-101-6512-16 for 16 pages of tables. Order by PAPS number and journal reference from American Institute of Physics, Physics Auxiliary Publication Service, Carolyn Gehlbach, 500 Sunnyside Boulevard., Woodbury, New York 11797-2999. The price is $1.50 for each microfiche (98 pages) or $5.00 for photocopies of up to 30 pages, and $0.15 for each additional page over 30 pages. Airmail additional. Make checks payable to the American Institute of Physics.
[18] C. C. Costain, J. Chem. Phys. **29**, 864 (1958); M. D. Harmony, V. W. Laurie, R. L. Kuczkowski, R. H. Schwendeman, and D. A. Ramsay, J. Phys. Chem. Ref. Data. **8**, 619 (1979).
[19] A. Bondi, J. Phys. Chem. **68**, 441 (1964).
[20] J. T. Hougen, J. Mol. Spectros. **114**, 395 (1985); L. H. Coudert and J. T. Hougen, *ibid.* **130**, 86 (1988).
[21] D. F. Plusquellic, X.-Q. Tan, and D. W. Pratt, J. Chem. Phys. **96**, 8026 (1992).
[22] D. D. Nelson, Jr., W. Klemperer, G. T. Fraser, F. J. Lovas, and R. D. Suenram, J. Chem. Phys. **87**, 6365 (1987); J. G. Loeser, C. A. Schmuttenmaer, R. C. Cohen, M. J. Elrod, D. W. Steyert, R. J. Saykally, R. E. Bumgarner, and G. A. Blake, *ibid.* **97**, 4727 (1992).
[23] X-Q. Tan and D. W. Pratt, J. Chem. Phys. **100**, 7061 (1994).
[24] D. F. Eggers (private communication).
[25] A. Held and D. W. Pratt, J. Am. Chem. Soc. **115**, 9718 (1993).
[26] A. D. Buckingham and P. W. Fowler, Can. J. Chem. **63**, 2018 (1985).
[27] L.-W. Xu, A. Taleb-Bendiab, L. Nemes, and R. L. Kuczkowski, J. Am. Chem. Soc. **115**, 5723 (1993).
[28] R. D. Amos and J. E. Rice, *The Cambridge Analytic Derivatives Package, Issue 4.0* (Cambridge University Press, Cambridge, 1987).
[29] E. J. Goodwin and A. C. Legon, J. Chem. Phys. **85**, 6828 (1986).
[30] E. B. Wilson, Jr., J. C. Decivs, and P. C. Cross, *Molecular Vibrations* (Dover, New York, 1955).